Persistent Infection of SARS Coronavirus in Colonic Cells In Vitro

Paul K.S. Chan,[1,2]* **Ka-Fai To,**[3] **Anthony W.I. Lo,**[3] **Jo L.K. Cheung,**[2] **Ida Chu,**[2] **Florence W.L. Au,**[3]
Joanna H.M. Tong,[3] **John S. Tam,**[1,2] **Joseph J.Y. Sung,**[1] **and Ho-Keung Ng**[3]

[1]*Centre for Emerging Infectious Diseases, The Chinese University of Hong Kong, Prince of Wales Hospital, Shatin,
New Territories, Hong Kong SAR, China*
[2]*Department of Microbiology, The Chinese University of Hong Kong, Prince of Wales Hospital, Shatin, New Territories,
Hong Kong SAR, China*
[3]*Department of Anatomical and Cellular Pathology, The Chinese University of Hong Kong, Prince of Wales Hospital,
Shatin, New Territories, Hong Kong SAR, China*

Severe acute respiratory syndrome coronavirus (SARS-CoV) can produce gastrointestinal symptoms. The intestinal tract is the only extrapulmonary site where viable viruses have been detected. This study examined seven established human intestinal cell lines, DLD-1, HCT-116, HT-29, LoVo, LS-180, SW-480 and SW-620, for their permissiveness to SARS-CoV infection. The results showed that only LoVo cells were permissive to SARS-CoV infection as evident by positive findings from indirect immunofluorescence staining for intracellular viral antigens, in situ hybridization for intracellular viral RNA, and electron microscopy for intracellular viral particles. In contrast to Vero cells, SARS-CoV did not produce cytopathic effects on LoVo cells. However, LoVo cells were found to be highly permissive for productive infection with a high viral titre ($>3 \times 10^7$ viral copies/ml) produced in culture supernatant following a few days of incubation. SARS-CoV established a stable persistent chronic infection that could be maintained after multiple passages. Being a cell line of human origin, LoVo cells could be a useful in vitro model for studying the biology and persistent infection of SARS-CoV. Our results on the expression of angiotensin-converting enzyme 2 (ACE2), a recently identified cellular receptor for SARS-CoV, in these cell lines indicated that it might not be the sole determinant for cells to be susceptible to SARS-CoV infection. *J. Med. Virol. 74:1–7, 2004.* © 2004 Wiley-Liss, Inc.

KEY WORDS: SARS; coronavirus; persistent infection; in vitro; receptor; ACE2

INTRODUCTION

Severe acute respiratory syndrome (SARS) is a newly emerged human disease caused by a novel coronavirus (SARS-CoV) [Drosten et al., 2003; Ksiazek et al., 2003; Peiris et al., 2003a]. SARS was first identified from Southern China in November 2002. Up to July 2003 when the global outbreak came to a halt, a total of 8,098 cases had been reported to the World Health Organization [WHO, 2003]. SARS in adult is characterized by an acute onset of fever with subsequent progression to pneumonia [Chan et al., 2003; Lee et al., 2003; Poutanen et al., 2003], whereas infection in children usually presents as a mild upper respiratory tract illness [Hon et al., 2003]. The causative agent, SARS-associated coronavirus (SARS-CoV) is phylogenetically distinct from previous known human and animal coronaviruses [Marra et al., 2003; Rota et al., 2003]. SARS-CoV does not grow in cell lines used commonly for isolating respiratory viruses, such as Hep2, HeLa, Madin-Darby Canine kidney (MDCK) and LLC-MK2 [Chan et al., 2003], but produce readily lytic infection in African Green monkey (Vero) cells [Chan et al., 2003; Ng et al., 2003a,b]. While SARS-CoV is notorious for producing

severe respiratory tract disease, a substantial proportion of patients had concurrent gastrointestinal symptoms [Lee et al., 2003; Leung et al., 2003; Peiris et al., 2003b]. SARS-CoV was found in intestinal biopsy samples taken during the early phase of the illness [Leung et al., 2003]. Studies on fatal cases also demonstrated that the gastrointestinal tract was the only extra-pulmonary site where viable viruses could be found [To et al., 2004].

The pathogenesis of SARS-associated diseases remained elusive. Although viable viruses could be found in lung and intestinal tissues, the pathology of the lung was different from those of the gastrointestinal tract [To et al., 2004; Tse et al., 2004]. While the SARS-CoV-infected lung was dominated by a diffuse alveolar damage picture with giant cell and atypical pneumocyte formations, the gastrointestinal tract appeared intact and syncytium-forming giant cells were not seen [Tse et al., 2004].

At present, a human cell-derived culture model for SARS-CoV is not available. Here, we report our findings on searching for human intestinal cell lines that may represent a more appropriate model for studying the biology of SARS-CoV.

MATERIALS AND METHODS

Cell Lines and Viruses

Seven human colorectal adenocarcinoma cell lines were investigated for their permissiveness to SARS-CoV infection. These cell lines were originally obtained from American Type Culture Collection (ATCC, Manassas, VA) and maintained with the recommended medium (Table I). The CUHK-W1 strain of SARS-CoV (GenBank accession no. AY278554) was grown in Vero cells and the third passage at a concentration of 5×10^6 50% tissue culture infective doses (TCID_{50})/ml was kept at $-70°C$ for experiments.

Cell lines at $60-70\%$ confluence in 25-cm^2 flasks were inoculated with 300 µl of virus suspension to provide a multiplicity of infection (MOI) of 10. Inoculated cell cultures were incubated at $37°C$. A mock infection was performed in parallel for each cell line. The cell monolayers were examined daily for cytopathic effects. Cells were harvested after seven days of incubation for virus detection.

Indirect Immunofluorescence Assay

Intracellular viral antigens were detected by indirect immunofluorescence staining based on a convalescent serum collected from a SARS patient as previously described [Chan et al., 2004a]. Briefly, cells were spotted onto a 12-well Teflon-coated glass microscope slides, and fixed with 100% pre-chilled acetone. A 25-µl aliquot of the 1:160 diluted convalescent serum was placed on the coated wells, and incubated at $37°C$ for 30 min in a moist chamber. After washing, a fluorescein isothiocyanate (FITC)-conjugated rabbit anti-human IgG antibody (Dako, Glostrup, Denmark) was added at a dilution of 1:40, and incubated for 30 min at $37°C$. Epifluorescence microscopy was performed on a Zeiss Axoplan 2 microscope equipped with the appropriate sets of excitation and emission filters. Grey scale images were captured by a cooled charge-coupled device.

Fluorescence In Situ Hybridization

Intracellular viral RNA was detected by in situ hybridization based on a digoxigenin-labeled DNA probe targeting the putative membrane protein encoding region of SARS-CoV as previously described [To et al., 2004]. Briefly, formalin-fixed cell block sections were treated with microwave heating in 0.01M sodium citrate buffer, and then fixed in 4% paraformaldehyde. Hybridization was carried out at high stringency with DNA probe at a concentration of 2 ng/µl in 15 µl of hybridization mix (50% formamide, 10% dextran sulphate in 2× Saline Sodium Citrate [SSC]) at $42°C$ for 16 hr under 20×20 mm coverslips in a moist chamber. Excess probe was removed by washing in 2× SSC for 5 min at room temperature. This was followed by three times high stringency washes in 0.1× SSC for 10 min at $61°C$. Immunological detection was conducted with anti-digoxigenin-rhodamine (Roche, Indianapolis, IN) following the manufacturer's instruction, and counterstained with 4,6 diamindino-2-phenylindol (DAPI) in an anti-fade mountant (Vectorshield, Vector Laboratory, Burlingame, CA). Cell block preparations from SARS-CoV-infected and non-infected Vero cell culture were used as positive and negative controls, respectively. The signal specificity was assessed by digestion of the sections with RNase A prior to hybridization, and by omission of the probes in the hybridization mixture.

TABLE I. Human Colorectal Adenocarcinoma Cell Lines Used for SARS-CoV Inoculation

Cell line	ATCC number	Growth medium
DLD-1	CCL-221	RPMI 1640, 10% fetal bovine serum
HCT-116	CCL-247	McCoy's 5a medium, 1.5 mM L-glutamine, 1.5 g/L sodium bicarbonate, 10% foetal bovine serum
HT-29	HTB-38	McCoy's 5a medium, 10% foetal bovine serum
LoVo	CCL-229	Ham's F12K medium, 10% foetal bovine serum
LS-180	CL-187	Eagle's minimum essential medium, 10% fetal bovine serum
SW-480	CCL-228	L-15 medium, 10% foetal bovine serum
SW-620	CCL-227	L-15 medium, 10% foetal bovine serum

ATCC, American Type Culture Collection, Manassas, VA.

Electron Microscopy

Cell pellets harvested after 7 days of incubation were fixed in 2.5% glutaraldehyde in 0.1M phosphate buffer (pH 7.2), and processed for examination by transmission electron microscopy.

Real Time RT-PCR Assay

Further experiments were undertaken on LoVo cells as they were the only cells found to be permissive to SARS-CoV. Cell culture flasks containing LoVo cells at 60–70% confluence were inoculated with SARS-CoV at 10, 1 and 0.1 MOI, respectively. The concentration of virus in cell culture supernatant was monitored by real time reverse transcription polymerase chain reaction (RT-PCR). Aliquots of 140 µl cell culture supernatant were collected daily for RNA extraction using the Qiagen RNA Mini Kit (Qiagen, Hilden, Germany). One-step real time quantitative RT-PCR was carried out using primers Pol-1 5′-AGC TCG CGT CTC AGT TTC AAG-3′ and Pol-2 5′-TGC CAG AAG CTG CAT GCA-3′ targeting the orf1ab polyprotein of SARS-CoV (nt 14442–14511 of strain CUHK-W1, GenBank accession no. AY278554); and TaqMan MGB probe 5′-(FAM)-GAT CAG CAG CAT ACA ACT-(MGBNFQ)-3′. The RT-PCR reactions were set up using the TaqMan® EZ RNA PCR reagent kit, (Applied Biosystems, Foster City, CA) following the manufacturer's protocol. Samples, reaction controls and standards were tested in duplicates. The thermal cycling parameters were optimized for the Sequence Detector 7700 (Applied Biosystems). The conditions were 50°C for 2 min for the activity of uracil N-glycosylase (UNG), followed by reverse transcription at 60°C for 30 min, inactivation of UNG at 95°C for 5 min, then 40 cycles of 94°C for 20 sec and 60°C for 1 min.

The infected LoVo cell cultures were split at a ratio of 1:4 after every 7 days of incubation, and continued for a total of seven passages. The proportion of infected cells obtained at the end of each passage was assessed by immunofluorescence staining, and with the concentration of virus in culture supernatant assessed by real time RT-PCR.

ACE2 Expression

The expression of angiotensin-converting enzyme 2 (ACE2) in these cell lines was examined as described previously [Harmer et al., 2002]. Briefly, total RNA was extracted using Qiagen RNeasy kit (Qiagen) according to the manufacturer's instructions. cDNA was synthesized from 2 µg of total RNA using Superscript III reverse transcriptase (Invitrogen, Carlsbad, CA) with random primers. The expression level of ACE2 mRNA was determined by real time RT-PCR using the TaqMan® EZ RNA PCR reagent kit (Applied Biosystems). Variations in input RNA amounts were compensated by measuring the RNA level of a housekeeping gene, beta-actin. The sequences of the primers and probes were as follows: ACE2 forward primer: 5′-CAT TGG AGC AAG TGT TGG ATC TT-3′; ACE2 reverse primer: 5′-GAG

CTA ATG CAT GCC ATT CTC A-3′; ACE2 probe: 5′-(FAM)-CTT GCA GCT ACA CCA GTT CCC AGG CA (TAMRA)-3′; beta-actin forward primer: 5′-CTG GCA CCC AGC ACA ATG-3′; beta-actin reverse primer: 5′-GCC GAT CCA CAC GGA GTA CT-3′; beta-actin probe: 5′-(VIC)-TCA AGA TCA TTG CTC CTC CTG AGC GC-(TAMRA)-3′. The PCR and thermal cycling conditions were as described previously [Harmer et al., 2002]. The relative expression of ACE2 of different cell lines were analyzed using the comparative threshold cycle (C_T) method as detailed in the ABI PRISM 7700 Sequence Detection System User Bulletin Number 2. Briefly, the ΔC_T for each sample was calculated by subtracting the average C_T of beta-actin from the average C_T of ACE2. The cell line with the lowest ACE2 expression level was used as a reference for calculating $\Delta\Delta C_T$, which was obtained by subtracting $\Delta C_{T(reference)}$ from $\Delta C_{T(sample)}$. The relative quantitation was then calculated by $2^{-\Delta\Delta C_T}$. The mRNA quantity for the reference cell line was expressed as 1.0, and all other quantities were expressed as a number of fold differences relative to the reference cell line.

RESULTS

Susceptibility of LoVo Cells to SARS-CoV Infection

Seven established cell lines of human intestinal origin, DLD-1, HCT-116, HT-29, LoVo, LS-180, SW-480 and SW-620, were investigated for their permissiveness to SARS-CoV infection. None of them showed cytopathic effects during the 7 days of incubation. Fluorescence in situ hybridization (FISH) and indirect immunofluorescence staining revealed the presence of SARS-CoV in LoVo cells, whereas all other cell lines were virus-free after 7 days of incubation. Viral genome was detected in the cytoplasm of infected LoVo cells by FISH using a probe specific to the putative M protein encoding region. For the FISH, positive signals appeared as red fluorescence as shown in Figure 1. Perinuclear accentuation of positive signals was also observed. The nuclei of infected and non-infected LoVo cells appeared blue due to counter stain (Fig. 1). Indirect immunofluorescence staining also indicated the presence of viral antigens in the cytoplasm of infected LoVo cells. SARS-CoV antigens were appeared as fluorescence green, whereas the background appeared red due to counter stain (Fig. 2).

While no morphological changes of infected LoVo cells could be observed with light microscopy at magnification of 400×, ultrastructural changes resulting from viral infection were found when examined by electron microscopy. The infected cells contained cytoplasmic vesicles, consistent with dilated endoplasmic reticulum and Golgi apparatus, which were packed with numerous spherical viral cores at different stages of maturation as shown in Figure 3A,B. These cores contained both viral proteins and the genome of SARS-CoV. In addition, mature virus particles of sizes ranging from 80 to 120 nm were found on the outer surface of the plasma membrane
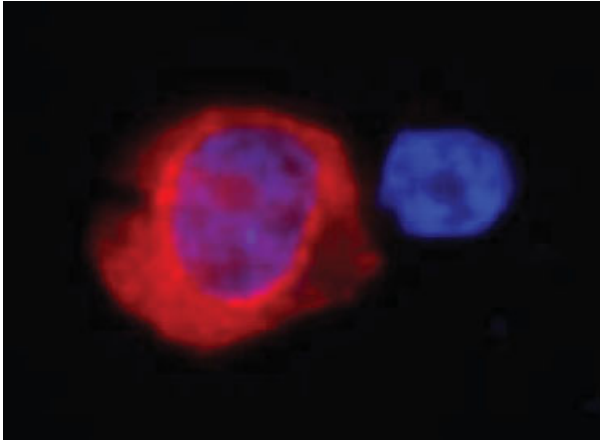
Fig. 1. Fluorescence in situ hybridisation (FISH). FISH carried out on a severe acute respiratory syndrome coronavirus (SARS-CoV)-infected LoVo cell block. On the left side of the figure, a SARS-CoV-infected LoVo cell showed red fluorescence signals in the cytoplasm indicating a positive FISH result. Peri-nuclear accentuation of signals in the infected cell was noted. No positive signal was seen on the uninfected cell on the right side. The nuclei are counter-stained with 4,6 diamindino-2-phenylindol (DAPI) and pseudo-coloured blue.

(Fig. 3C). Thus, FISH, indirect immunofluorescence and ultrastructural studies confirmed the permissiveness of LoVo cells to SARS-CoV infection.

Dynamics of SARS-CoV Infection in LoVo Cells

The concentration of viruses in the cell culture supernatants collected over the first week after virus inoculation is shown in Figure 4. The production of virus increased exponentially after 2–3 days of virus inoculation, and appeared in a dose-dependent manner. The infected LoVo cells sustained a persistent infection for all the passages that we had performed. At the end of each passage, about 50–60% of cells were infected as revealed by immunofluorescence staining, and a virus
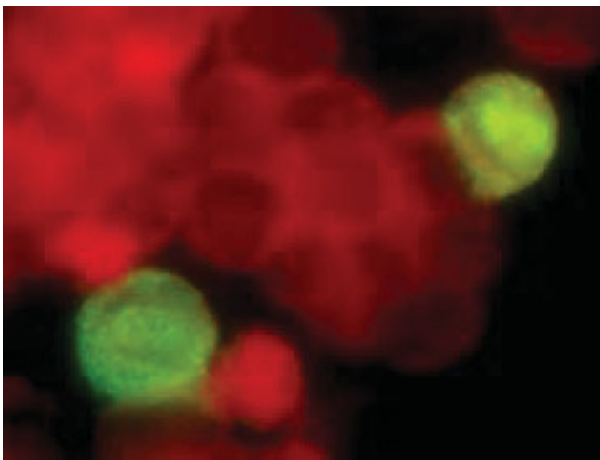

Fig. 2. Indirect immunofluorescence staining. Two SARS-CoV-infected LoVo cells with green fluorescence signals indicating positive indirect immunofluorescence staining results. Convalescent serum from SARS patient was used as the primary antibody. The cytoplasm was countered stained by Evan's blue.
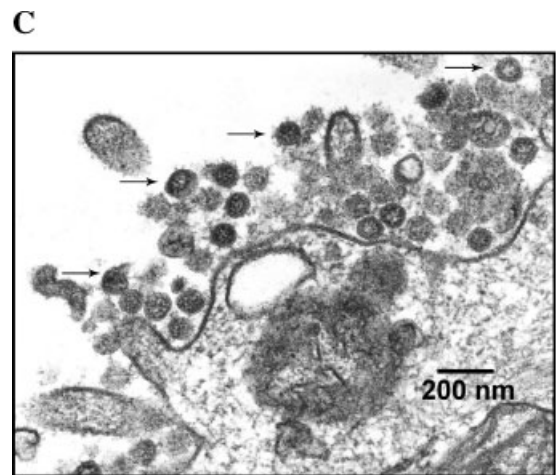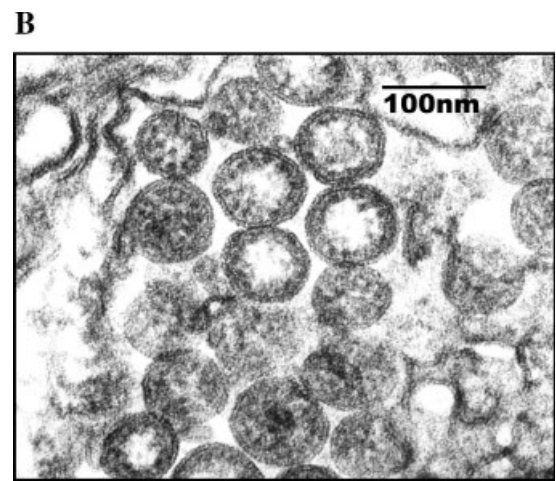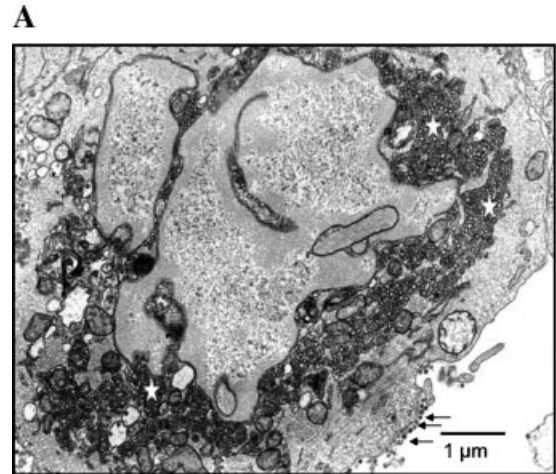

Fig. 3. Electron micrographs. **A**: Electron micrograph showing the nucleus and the adjacent cytoplasm of a SARS-CoV-infected LoVo cell. The coronavirus particles are packed in dilated spaces with a peri-nuclear accentuation pattern as indicated by white stars. The dilated cytoplasmic vesicles likely represent dilated endoplasmic reticulum and Golgi apparatus. Coronavirus particles are also seen along the cytoplasmic membrane as indicated by black arrows. **B**: Higher magnification showing coronavirus cores inside a dilated cytoplasmic vesicle. Viral core particles appear at different stages of maturation are seen. **C**: Higher magnification showing mature coronavirus particles along the outer surface of cytoplasmic membrane. The enveloped viral particles range from 80 to 120 nm. The characteristic pedal-shaped surface spikes are noted.
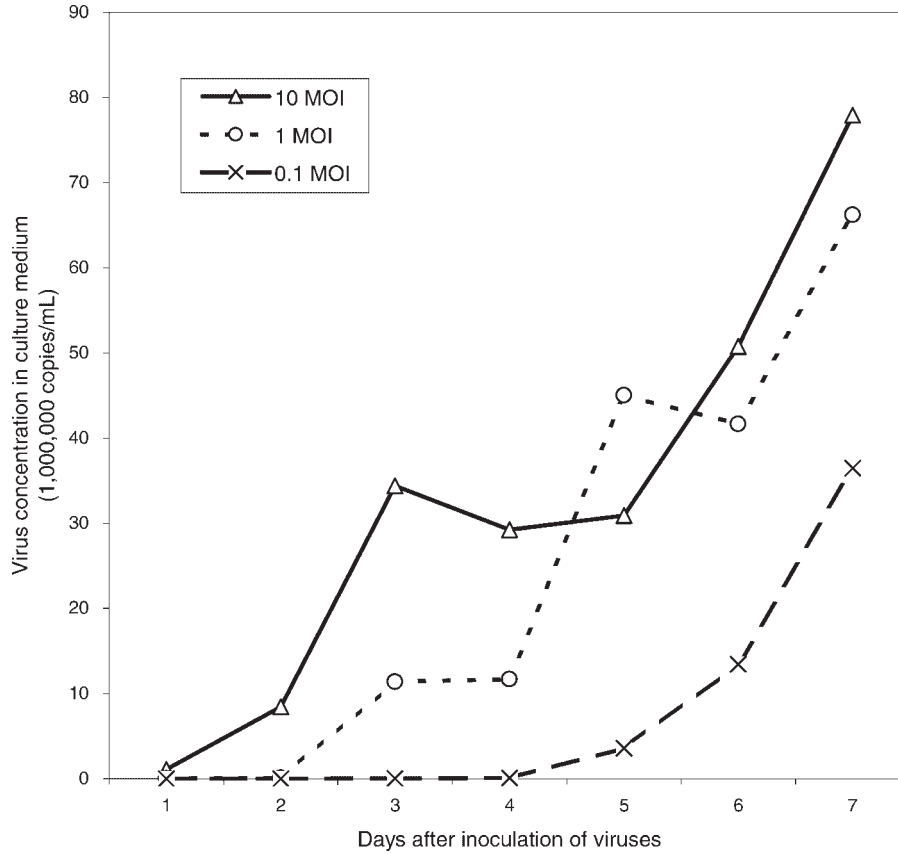
Fig. 4. Virus production from LoVo cells inoculated with SARS-CoV at different multiplicity of infection (MOI).

concentration in the range of $2-9 \times 10^7$ copies/ml was detected from the cell culture supernatant.

Expression of ACE2 in LoVo and Other Non-Permissive Cell Lines

In view of the current evidence of ACE2 as the cellular receptor for SARS-CoV, we investigated the relationship between permissiveness to SARS-CoV infection and ACE2 expression in these colorectal adenocarcinoma cell lines. Table II shows the results of relative expressional level of ACE2 using real time RT-PCR. Surprisingly, apart from LoVo cells, ACE2 was also found to be expressed in other cell lines that were not permissive to

TABLE II. Expression of Angiotensin Converting Enzyme 2 (ACE2) in Human Colorectal Adenocarcinoma Cell Lines

Cell line	ΔC_T of ACE2[a]	No. of fold difference in ACE2 expression relative to HCT-116[b]
HCT-116	15.23	1.0
DLD-1	13.40	3.54
HT-29	12.88	5.08
SW-480	12.69	5.80
LoVo	11.42	13.98
LS-180	8.56	101.83
SW-620	5.78	699.41

[a]C_T Threshold cycle; ΔC_T = average $C_{T(ACE2)}$ − average $C_{T(beta-actin)}$.
[b]Calculated by $2^{-\Delta\Delta C_T}$, where $\Delta\Delta C_T = \Delta C_{T(sample)} - \Delta C_{T(HCT-116)}$.

SARS-CoV infection. Remarkably, the cell lines LS-180 and SW620 expressing high levels of ACE2 mRNA were found to be non-permissive to SARS-CoV infection.

DISCUSSION

Our results showed that the human colorectal adenocarcinoma-derived LoVo cell line was susceptible to SARS-CoV infection. SARS-CoV produced a persistent infection in LoVo cells, and the infection could be maintained after multiple passages. SARS-CoV did not produce observable cytopathic effects on LoVo cells at the microscopic level. This is in stark contrast to Vero cells, where SARS-CoV produced a lytic infection with characteristic refractile rounding cytopathic effects [Ng et al., 2003a,b]. The fact that SARS-CoV did not produce lytic infection in this intestinal cell line is reminiscence of what we have observed from the endoscopic intestinal biopsies obtained from a SARS patient [Leung et al., 2003], and in fatal cases of SARS [To et al., 2004]. Although viral particles inside the ileal and colonic epithelial cells were revealed by electron microscopy, the SARS-CoV-infected ileal and colonic mucosa appeared normal at microscopic level and no viral inclusion bodies could be detected. Multinucleated pneumocytes were observed in SARS-CoV-infected lungs in human and monkey models [Fouchier et al., 2003; Kuiken et al., 2003; To et al., 2004], and formation

REFERENCES

Chan PKS, Tam JS, Lam CW, Chan E, Wu A, Li CK, Buckley TA, Ng KC, Joynt GM, Cheng FWT, To KF, Lee N, Hui DS, Cheung JL, Chu I, Liu E, Chung SS, Sung JJY. 2003. Human metapneumovirus detection in patients with severe acute respiratory syndrome. Emerg Infect Dis 9:1058–1063.

Chan PKS, Ng KC, Chan RCW, Lam RKY, Chow VCY, Hui M, Wu A, Lee N, Yap HY, Cheng FWT, Sung JJY, Tam JS. 2004a. Immunofluorescence assay for serologic diagnosis of SARS. Emerg Infect Dis 10:530–532.

Chan PKS, To WK, Ng KC, Lam RKY, Ng TK, Chan RCW, Wu A, Yu WC, Lee N, Hui DSC, Lai ST, Hon EKL, Li CK, Sung JJY, Tam JS. 2004b. Laboratory Diagnosis of SARS. Emerg Infect Dis 10:825–831.

Drosten C, Gunther S, Preiser W, van der WS, Brodt HR, Becker S, Rabenau H, Panning M, Kolesnikova L, Fouchier RA, Berger A, Burguiere AM, Cinatl J, Eickmann M, Escriou N, Grywna K, Kramme S, Manuguerra JC, Muller S, Rickerts V, Sturmer M, Vieth S, Klenk HD, Osterhaus AD, Schmitz H, Doerr HW. 2003. Identification of a novel coronavirus in patients with severe acute respiratory syndrome. N Engl J Med 348:1967–1976.

Fouchier RA, Kuiken T, Schutten M, van Amerongen G, van Doornum GJ, van den Hoogen BG, Peiris M, Lim W, Stohr K, Osterhaus AD. 2003. Aetiology: Koch's postulates fulfilled for SARS virus. Nature 423:240.

Harmer D, Gilbert M, Borman R, Clark KL. 2002. Quantitative mRNA expression profiling of ACE 2, a novel homologue of angiotensin converting enzyme. FEBS Lett 532:107–110.

Hon KLE, Leung CW, Cheng WT, Chan PKS, Chu WCW, Kwan YW, Li AM, Fong NC, Ng PC, Chiu MC, Li CK, Tam JS, Fok TF. 2003. Clinical presentations and outcome of severe acute respiratory syndrome in children. Lancet 361:1701–1703.

Ksiazek TG, Erdman D, Goldsmith CS, Zaki SR, Peret T, Emery S, Tong S, Urbani C, Comer JA, Lim W, Rollin PE, Dowell SF, Ling AE, Humphrey CD, Shieh WJ, Guarner J, Paddock CD, Rota P, Fields B, DeRisi J, Yang JY, Cox N, Hughes JM, LeDuc JW, Bellini WJ, Anderson LJ. 2003. A novel coronavirus associated with severe acute respiratory syndrome. N Engl J Med 348:1953–1966.

Kuiken T, Fouchier RAM, Schutten M, Rimmelzwaan GF, van Amerongen G, van Riel D, Laman JD, de Jong T, van Doornum G, Lim W, Ling AE, Chan PKS, Tam JS, Zambon MC, Gopal R, Drosten C, van der WS, Escriou N, Manuguerra JC, Stohr K, Peiris JSM, Osterhaus ADME. 2003. Newly discovered coronavirus as the primary cause of severe acute respiratory syndrome. Lancet 362: 263–270.

Lee N, Hui D, Wu A, Chan P, Cameron P, Joynt GM, Ahuja A, Yung MY, Leung CB, To KF, Lui SF, Szeto CC, Chung S, Sung JJY. 2003. A major outbreak of severe acute respiratory syndrome in Hong Kong. N Engl J Med 348:1986–1994.

Leung WK, To KF, Chan PKS, Chan HL, Wu AK, Lee N, Yuen KY, Sung JJY. 2003. Enteric involvement of severe acute respiratory syndrome-associated coronavirus infection. Gastroenterology 125: 1011–1017.

Li W, Moore MJ, Vasilieva N, Sui J, Wong SK, Berne MA, Somasundaran M, Sullivan JL, Luzuriaga K, Greenough TC, Choe H, Farzan M. 2003. Angiotensin-converting enzyme 2 is a functional receptor for the SARS coronavirus. Nature 426:450–454.

Marra MA, Jones SJ, Astell CR, Holt RA, Brooks-Wilson A, Butterfield YS, Khattra J, Asano JK, Barber SA, Chan SY, Cloutier A, Coughlin SM, Freeman D, Girn N, Griffith OL, Leach SR, Mayo M, McDonald H, Montgomery SB, Pandoh PK, Petrescu AS, Robertson AG, Schein JE, Siddiqui A, Smailus DE, Stott JM, Yang GS, Plummer F, Andonov A, Artsob H, Bastien N, Bernard K, Booth TF, Bowness D, Czub M, Drebot M, Fernando L, Flick R, Garbutt M, Gray M, Grolla A, Jones S, Feldmann H, Meyers A, Kabani A, Li Y, Normand S, Stroher U, Tipples GA, Tyler S, Vogrig R, Ward D, Watson B, Brunham RC, Krajden M, Petric M, Skowronski DM, Upton C, Roper RL. 2003. The Genome sequence of the SARS-associated coronavirus. Science 300:1399–1404.

Ng ML, Tan SH, See EE, Ooi EE, Ling AE. 2003a. Proliferative growth of SARS coronavirus in Vero E6 cells. J Gen Virol 84:3291–3303.

Ng ML, Tan SH, See EE, Ooi EE, Ling AE. 2003b. Early events of SARS coronavirus infection in vero cells. J Med Virol 71:323–331.

Peiris JS, Lai ST, Poon LL, Guan Y, Yam LY, Lim W, Nicholls J, Yee WK, Yan WW, Cheung MT, Cheng VC, Chan KH, Tsang DN,

of multinucleated syncytia was also observed in human fibroblast 293T cells rendered permissive by ACE2 transfection [Li et al., 2003]. However, multinucleated syncytium was not observed in SARS-CoV-infected LoVo cells. This observation accords the histopathological findings in intestinal biopsies and autopsy specimens obtained from SARS patients [Leung et al., 2003; To et al., 2004].

The current finding of persistent infection in colonic cells in vitro is in line with the clinical observation of prolonged shedding of SARS-CoV in stool samples. It has been reported that shedding of SARS-CoV in stool for 3–4 weeks after the onset of illness was common, and prolonged shedding for more than 2 months occurred in some patients [Chan et al., 2004b]. The use of a non-lytic productive cycle by the virus in cultured intestinal cell lines may provide a biological basis for these clinical observations.

Our data from the previous outbreak showed that only 30% of RT-PCR-positive nasophayngeal/tracheal aspirate samples, and <1% of RT-PCR-positive stool samples had viruses isolated by Vero E6 cells [Chan et al., 2004b]. The reasons for the poor sensitivity of Vero E6 cells in detecting SARS-CoV are not entirely clear. On one hand, cell culture-based assay requires intact and functional viral particles while nucleic acid-based method requires only a partial viral genome. On the other hand, species and tissue type differences may play a significant role in the overall sensitivity of the cell culture-based method. Our results show that LoVo cells can serve as an alternative human cell line for virus isolation. It is worthwhile to investigate whether LoVo cells could provide a more sensitive system for isolating SARS-CoV from clinical samples. LoVo cells, being an immortalized adenocarcinoma cell line, also have the advantages of fast doubling time and requiring relatively simple culture media to maintain. In addition, LoVo cells being originated from human, appears to recapture, at least partially, the biological consequences of the intestinal epithelium following infection with SARS CoV. The LoVo cells could potentially be a useful model for the in vitro study of the pathogenesis of SARS-CoV-related diseases.

Recently, ACE2 has been shown to be the cellular receptor for SARS-CoV in Vero E6 cells [Li et al., 2003; Wong et al., 2004]. Apart from the cardiovascular system and kidney, intestinal tissues were also shown to express high levels of ACE2 [Harmer et al., 2002]. Our results indicated that ACE2 was expressed in all the seven adenocarcinoma cell lines investigated. The ACE2 expression level of LoVo cells was intermediate as compared to others (Table II). However, only the LoVo cells were found to be permissive to SARS-CoV infection. These results indicate that ACE2, by itself, is insufficient to explain the infectivity of SARS-CoV in intestinal cells. Hence, other cellular factors may play a role in completing the full life cycle of SARS-CoV. The possible factors that determine the susceptibility of different cell types to SARS-CoV infection deserve further investigations.

Yung RW, Ng TK, Yuen KY. 2003a. Coronavirus as a possible cause of severe acute respiratory syndrome. Lancet 361:1319–1325.

Peiris JS, Chu CM, Cheng VC, Chan KS, Hung IF, Poon LL, Law KI, Tang BS, Hon TY, Chan CS, Chan KH, Ng JS, Zheng BJ, Ng WL, Lai RW, Guan Y, Yuen KY. 2003b. Clinical progression and viral load in a community outbreak of coronavirus-associated SARS pneumonia: A prospective study. Lancet 361:1767–1772.

Poutanen SM, Low DE, Henry B, Finkelstein S, Rose D, Green K, Tellier R, Draker R, Adachi D, Ayers M, Chan AK, Skowronski DM, Salit I, Simor AE, Slutsky AS, Doyle PW, Krajden M, Petric M, Brunham RC, McGeer AJ. 2003. Identification of severe acute respiratory syndrome in Canada. N Engl J Med 348:1995–2005.

Rota PA, Oberste MS, Monroe SS, Nix WA, Campagnoli R, Icenogle JP, Penaranda S, Bankamp B, Maher K, Chen MH, Tong S, Tamin A, Lowe L, Frace M, DeRisi JL, Chen Q, Wang D, Erdman DD, Peret TC, Burns C, Ksiazek TG, Rollin PE, Sanchez A, Liffick S, Holloway B, Limor J, McCaustland K, Olsen-Rasmussen M, Fouchier R, Gunther S, Osterhaus AD, Drosten C, Pallansch MA, Anderson LJ, Bellini WJ. 2003. Characterization of a novel coronavirus associated with severe acute respiratory syndrome. Science 300:1394–1399.

To KF, Tong JHM, Chan PKS, Au FWL, Chim SSC, Chan AKC, Cheung JLK, Liu EYM, Tse GMK, Lo AWI, Lo DYM, Ng HK. 2004. Tissue and cellular tropisms of the coronavirus associated with Severe Acute Respiratory Syndrome—An in-situ hybridization study of fatal cases. J Pathol 202:157–163.

Tse GMK, To KF, Chan PKS, Lo AWI, Ng KC, Wu A, Lee N, Wong HC, Mak SM, Chan KF, Hui DSC, Sung JJY, Ng HK. 2004. Pulmonary pathological features in coronavirus associated severe respiratory syndrome (SARS). J Clin Pathol 57:260–265.

Wong SK, Li W, Moore MJ, Choe H, Farzan M. 2004. A 193-amino-acid fragment of the SARS coronavirus S protein efficiently binds angiotensin-converting enzyme 2. J Biol Chem 279:3197–3201.

World Health Organization. 2003. Summary of probable SARS cases with onset of illness from 1 November 2002 to 31 July 2003 (revised 25 September 2003) http://www.who.int/csr/sars/country/table2003_09_23/en/print.html (assessed on 30 December 2003).